GLOBAL BIOGEOCHEMICAL CYCLES, VOL. 9, NO. 1, PAGES 153–166, MARCH 1995

Distribution of radiocarbon as a test of global carbon cycle models

Atul K. Jain,[1,4] Haroon S. Kheshgi,[2] Martin I. Hoffert,[3] and Donald J. Wuebbles[1,4]

Abstract. Accurate global carbon cycle models are needed to estimate the future change of atmospheric CO_2 for specified scenarios of CO_2 emissions. Model accuracy cannot be tested directly because of the difficulty in estimating the carbon flux to the oceans and the terrestrial biosphere. However, one test of model consistency is the requirement that the model reproduce past changes and spatial distributions of ^{14}C. A model for carbon exchange within and among the atmosphere, oceans, and terrestrial biosphere is found to satisfy this test. The ocean is modeled as an upwelling-diffusion column capped by a mixed layer with recirculation of the polar bottom water to complete the thermohaline circulation. This ocean advection scheme contains only two key dynamic parameters, the vertical eddy diffusivity κ and the upwelling velocity w, which are calibrated to match the vertical distribution of preanthropogenic ^{14}C. The thermocline depth scale κ/w = 1343 m found by calibration is considerably deeper than that required to match the steady vertical temperature profile (500 m). This is consistent with the hypothesis that isopycnal mixing, which is much more rapid than diapycnal mixing, has a stronger effect on ^{14}C than on temperature since isopycnals are nearly isothermal. This model is found to match measured values, within measurement error, of the prebomb decrease in ^{14}C in the atmosphere and the mixed layer due to the Suess effect, the bomb ^{14}C in the mixed layer, the bomb ^{14}C penetration depth, the bomb ^{14}C ocean inventory, and the vertical distribution of total carbon. Results are compared to those of other schematic carbon cycle models as well as those of ocean general circulation models.

Introduction

Ocean carbon cycle models calibrated to reproduce radiocarbon concentrations are playing an important role in estimating the future buildup of fossil fuel CO_2 in the atmosphere [*Toggweiler et al.*, 1989a,b; *Siegenthaler and Joos*, 1992; *Siegenthaler and Sarmiento*, 1993]. A primary motivation for tracer calibration of ocean carbon cycle models is the difficulty (associated with buffering by ocean carbonate chemistry) of directly measuring the uptake of carbon dioxide by the oceans. A hierarchy of such models has developed over the years. Computational considerations, internal consistency, and a given model's ability to reproduce observations are key factors in selecting a model type for a given application.

The earliest carbon cycle models were of the classical multibox type [*Revelle and Suess*, 1957; *Bolin and Eriksson*, 1959; *Broecker et al.*, 1971; *Machta*, 1973; *Hoffert*, 1974; *Keeling*, 1973, 1977; *Bacastow and Keeling*, 1973; *Bjorkstrom*, 1979; *Broecker and Peng*, 1982]. These offer an intuitively appealing approach to finding the time variation of the mass $N_i(t)$ of stable carbon isotopes (^{12}C or ^{13}C) or radiocarbon (^{14}C) in each of a number of well-mixed reservoirs in response to a specified carbon emission rate $N_i(t)$. Multibox models normally assume first-order transport kinetics in which the outflux from box i to some adjacent box j is $k_{ij}N_i$ leading to reservoir differential equations of the form

$$\frac{dN_i}{dt} = \sum_{i=1}^{n}(k_{ji}N_j - k_{ij}N_i) + \dot{N}_i - \lambda N_i$$

where n is the number of boxes. The term $-\lambda N_i$ applies to radiocarbon decay, where $\lambda = 1.21 \times 10^{-4}$ yr^{-1} is the decay constant for $^{14}C \rightarrow {}^{14}N + \beta^- + \nu$. Exchange coefficients k_{ij} ($i \neq j$) have inverse time units and are normally calibrated to recover observed carbon masses (or concentrations) of the reservoirs in the steady state ($dN_i/dt = 0$). The number of boxes and the disaggregation scheme for the oceans are somewhat at the discretion of the modeler. The minimum box number is three: an atmosphere ($i = a$), an ocean mixed layer ($i = m$), and a deep ocean ($i = d$). Single box oceans cannot make realistic projections of future CO_2 levels because carbon uptake is not limited by CO_2 gas exchange at the atmosphere-mixed layer interface but by deeper thermocline mixing. This is modeled to a first approximation by the k_{md} coefficient.

High-latitude box models [*Sarmiento and Toggweiler*, 1984; *Siegenthaler and Wenk*, 1984; *Knox and McElroy*, 1984; *Volk and Liu*, 1988; *Toggweiler and Sarmiento*, 1985] with separate polar- and nonpolar-mixed layer boxes were proposed to explain atmospheric CO_2 variations during glacial-interglacial transitions thought to arise from ocean composition changes pumped by circulation, solubility, or biology changes [*Volk and Hoffert*, 1985]. Inclusion of a polar box addresses this problem by

[1] Lawrence Livermore National Laboratory, Livermore, California.
[2] Exxon Research and Engineering Company, Annandale, New Jersey.
[3] Department of Earth Systems Science, New York University, New York.
[4] Now at University of Illinois, Urbana

Paper number 94GB02394.
0886-6236/95/94GB-02394$10.00

estimating the effect of composition variations in polar surface waters on the strength of the ocean CO_2 sink. However, present models show too small an effect. How did atmospheric CO_2 increase from the midst of the last glaciation to the preindustrial concentration of 278 parts per million by volume (ppmv) by the ice-core-recorded 80 ppmv? And how were ocean carbon pump changes triggered by Milankovitch changes in solar radiation over the seasons and latitudes? These remain open questions that are being actively studied.

If one divides the oceans into enough boxes, the result mimics a finite difference model of the three-dimensional (3-D) oceans. Multiocean, multibox models [*Broecker and Peng*, 1986, 1987; *Bjorkstrom*, 1986; *Kier*, 1988, 1989; *Walker*, 1991; *Walker and Kasting*, 1992] are intermediate steps, distinguishing different water masses and ocean basins but falling short of full 3-D models. They typically use tracer-calibrated exchange coefficients as opposed to physical diffusivities, although they attempt to represent volumetric internal flows correctly. Box-diffusion models [*Oeschger et al.*, 1975; *Siegenthaler and Oeschger*, 1978; *Hoffert et al.*, 1979; *Keeling et al.*, 1989a,b] are a transition between discrete mutilayer ocean box models and vertically resolved continuous diffusion models. They do not include vertical advection or paths between the high-latitude surface ocean and the deep sea. The world's oceans are modeled by vertically stacked boxes of thickness Δz with two-way mass exchange between interior layers and their top and bottom neighbors. If the exchange coefficient between adjacent layers is constant, $k = k_{i,i+1} = k_{i,i-1}$, the effective diffusivity is $\kappa = k\Delta z^2$. Outcrop-diffusion and high-latitude exchange/interior diffusion-advection (HILDA) models [*Siegenthaler*, 1983; *Siegenthaler and Joos*, 1992; *Shaffer and Sarmiento*, 1994] combine diffusive models with discrete boxes in a manner meant to mimic the exchange of high-latitude surface ocean with the deep sea along constant potential density (isopycnal) outcrops. Upwelling-diffusion (UD) models [*Wyrtki*, 1962; *Munk*, 1966; *Hoffert et al.*, 1981; *Volk*, 1984; *Shaffer*, 1989; *Kheshgi et al.*, 1991] are vertically resolved ocean models including both upwelling and diffusion. Recent incarnations of UD models, including the one we develop in the present paper, allow for exchange with polar surface, deep oceans, and marine biosphere effects.

Ocean general circulation models of (OGCM) carbon cycle [*Sarmiento*, 1986; *Maier-Reimer and Hasselmann*, 1987; *Toggweiler et al.*, 1989a,b; *Maier-Reimer and Bacastow*, 1990; *Bacastow and Maier-Reimer*, 1990] are the most spatially detailed and computationally demanding treatments. They transport carbon within individual basins and around the world's oceans using 3-D current fields generated by the OGCMs; the internal 3-D circulation of oceans is very sparsely mapped by direct measurements. Sophisticated versions include a marine biosphere at a level of detail sufficient to track ecosystem dynamics [*Sarmiento et al.*, 1993]. The potential advantage of using a general circulation model (GCM) is that spatial distributions of both the data and model results can be compared to better constrain model parameters. However, OGCM circulations can depend on numerical integration schemes, model resolution, and input subgrid diffusivities [*Bryan*, 1987]. Their carbon uptake rates are also affected by mixing by unresolved eddies (which must be parameterized) and perhaps by spurious "numerical" diffusion.

A convolution integral of oceancarbon cycle model response to an impulsive injection of carbon can be used to find the response of the ocean carbon sink to changes in atmospheric concentration of CO_2 [*Maier-Reimer and Hasselmann*, 1987]. This approach can also be used to relate CO_2 emissions to atmospheric CO_2 concentrations in both direct and inverse modes [*Harvey*, 1989; *Wigley*, 1991]. However, it is accurate only so long as the governing equations remain nearly linear in the carbon variable. Variations in the oceanic carbonate buffer factor as emissions proceed may limit the applicability to small perturbations from the initial state (see below). In any case, one needs a believable carbon model to start with to generate the impulse response.

Prior comparisons have shown that simpler schematic models can predict present-day carbon uptake at rates comparable to OGCM-based carbon cycle models when normalized to recover the global mean penetration depth (in 1974) of bomb radiocarbon [*Siegenthaler and Sarmiento*, 1993]. These intercomparisons were made in preparation for an upcoming round of Intergovernmental Panel on Climate Change (IPCC) estimates of atmospheric CO_2 buildup projections from various carbon emission scenarios. However, the "simple" ocean carbon cycle models reported were limited to the box-diffusion and HILDA type.

An UD ocean carbon cycle model is one component of the global carbon cycle model shown in Figure 1 and developed in this paper. This model offers computational economy and a parameterization of ocean mixing consistent with the UD ocean energy balance model used by the IPCC [*Hoffert et al.*, 1980; *Bretherton et al.*, 1990] to estimate global greenhouse warming. In what follows, we discuss the physical significance of the model's mixing parameterization and develop the governing equations of an UD model for both stable and radioactive carbon isotopes. The model transport coefficients are calibrated so that model results for ^{14}C in the deep oceans match Geochemical Ocean Sections Study (GEOSECS) data. Model results are found to be consistent with the measured dilution of atmospheric ^{14}C by fossil fuel emissions (the Suess effect) and the penetration of the oceans by bomb-produced ^{14}C. The model is then used to calculate the historical buildup of atmospheric CO_2 including the effects of the land biosphere. *Siegenthaler and*

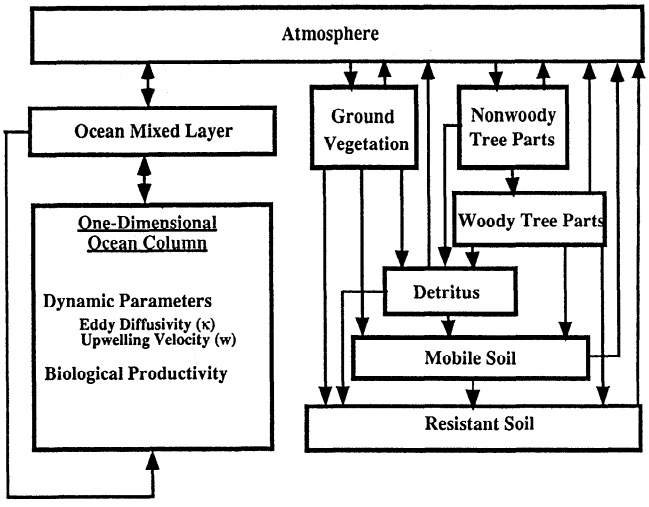

Figure 1. Diagram of the atmosphere-ocean-biosphere system model of the global carbon cycle.

Sarmiento's [1993] ocean carbon cycle uptake intercomparison is then extended to include our model results.

Ocean Chemistry and Transport

Uncertainties in oceanic carbon uptake rates arise mainly from uncertainties in how carbon mass is exchanged between the surface and the deep oceans. Carbon entering the oceans is "buffered" by rapid aqueous reactions to bicarbonate (HCO_3^-) and carbonate ions (CO_3^{-2}) in addition to dissolved carbon dioxide (CO_2). The relative concentrations of these constituents varies with the shifting equilibrium of the carbonate reactions. However, the concentration of dissolved inorganic carbon (DIC), $[CO_2] + [HCO_3^-] + [CO_3^{-2}]$, is conserved. Table 1 indicates the surface ocean DIC concentration and its partitioning for the preindustrial and present atmospheric CO_2 concentrations. Although atmospheric CO_2 (and atmospheric carbon mass) increased by 26.9% since preindustrial times, the change in DIC concentration of surface water is only 2.47%. The relative change in total ocean DIC is too small to measure over the entire ocean volume to construct an accurate estimate of the net ocean carbon uptake. For this reason carbon cycle models are tested by requiring that the model reproduce ^{14}C uptake and distribution. The ratio of these percentage changes is the present buffer factor, $\xi = 26.9/2.47 \approx 10.9$, defined in the appendix.

An effect of the biological productivity of surface-dwelling phytoplankton is the downward transport of carbon through the thermocline by the sinking of undecomposed particulate organic carbon (POC) and calcium carbonate shells (particulate inorganic carbon, PIC). Sinking POC is oxidized on the way down with the help of heterotropic bacteria and other organisms such as zooplankton to release CO_2 which appears as a DIC source. Excluding deepwater-forming regions at high-latitudes, the horizontally averaged oceans upwell at vertical velocity w. The downward biological carbon flux must be balanced in the steady state by upwelling and turbulent carbon fluxes, wC and $\langle w'C' \rangle$, where w' and C' are fluctuations in upwelling and concentration. A major parameter in our model is the eddy diffusivity, $\kappa = \langle w'C' \rangle / (\partial C/\partial z)$. When the surface concentration of DIC rises due to CO_2 transfer from the atmosphere, upward diffusion decreases and there is a net downward flux from the biological carbon rain.

Eddy diffusivity is not isotropic. The vertical component κ of eddy diffusivity is much small than the horizontal components. Order of magnitude calculations [*Hoffert and Flannery*, 1985] suggest that ubiquitous 50 to 100 km eddies [*Semtner and Chervin*, 1992] oriented along slightly inclined constant density surfaces (isopycnals) can produce eddy fluxes by isopycnal mixing whose vertical components are comparable to those of much smaller scale mixing across isopycnals (diapycnal mixing) by breaking internal gravity waves [*Sarmiento et al.*, 1982; *Redi*, 1982; *Kraus*, 1990). Slow vertical mixing, compared with CO_2 gas exchange at the surface, across the stably stratified thermocline is almost certainly the main bottleneck to oceanic fossil fuel carbon uptake. However, it is an open question whether isopycnal mixing, diapycnal mixing, or some combination is the dominant process responsible for vertical mixing.

A fundamental issue for schematic models is that the different values of eddy diffusivity can be found when the model is calibrated to reproduce the distribution of different tracers [*Siegenthaler and Joos*, 1992]. A possible explanation is that the relative contribution of isopycnal versus diapycnal mixing is different for different tracers if they have different patterns of surface penetration. For simplicity, and for consistency with prior ocean climate models, we take both κ and w as depth-independent constants at this point. Apart from mixing and upwelling through the thermocline, we also allow for a downward path for carbon through the polar sea as described below.

Table 1. Preindustrial and Present Concentrations of Dissolved Inorganic Carbon

	Preindustrial	Present	Change	Percent Change
pCO_2, μatm	279.0	354.1	75.1	26.9
$[CO_2]$, μmol kg^{-1}	9.3	11.8	2.5	26.9
$[CO_3^{--}]$, μmol kg^{-1}	215.8	185.5	-30.3	-14.0
$[HCO_3^-]$, μmol kg^{-1}	1711.9	1787.7	75.8	4.4
[DIC], μmol kg^{-1}	1937.0	1985.0	48.0	2.47

DIC = $[CO_2] + [CO_3^{--}] + [HCO_3^-]$ are shown for the surface ocean. Concentrations assumed to be at equilibrium with atmospheric CO_2 are computed for constant total alkalinity $[TA] = [HCO3^-] + 2[CO_3^{--}] + [H_2BO_3^-] + ... + [OH^-] - [H^+] =$ 2252 meqmol kg^{-1}, water temperature T_m = 19.2 °C and salinity S = 34.262‰ using the carbonate chemistry equilibrium constants given by *Peng et al.* [1987].

Model

The globally averaged model for carbon cycle depicted in Figure 1 consists of four reservoirs: the atmosphere, the terrestrial biosphere, the mixed layer of the ocean, and the deep ocean. The atmosphere and mixed layers are modeled as well-mixed reservoirs. The deep ocean, however, is treated as an advective-diffusive medium with a continuous distribution of DIC described by a one-dimensional (1-D) conservation of mass equation characterized by eddy diffusivity κ and upwelling velocity w [*Hoffert et al.*, 1981]. Although the oceanic thermohaline circulation is complex and not well understood [*Broecker and Peng*, 1982; *Toggweiler and Samuels*, 1993; *Caldeira et al.*, 1994], carbon cycle models which seek to investigate carbon storage in the ocean must characterize the effective transport properties of the circulating water masses. The approach we advocate in this paper is to utilize information from oceanographic tracer studies to calibrate transport coefficients for deep-sea transport. In our model the thermohaline circulation is schematically represented by polar deep water formation, with the return flow upwelling through the 1-D water column to the surface ocean from where it is returned, through the polar sea, as bottom water to the bottom of the ocean column thereby completing the thermohaline circulation. Bottom water formation and sinking have been observed in relatively restricted regions of the polar seas, while the return flow has not been

measured and must be inferred from ocean tracers or temperature. The effects of the return flow are expected to spread rapidly in the horizontal direction and are assumed to occur uniformly across the world ocean. This picture of large-scale thermohaline circulation of the world ocean (in which cold, dense seawater sinks at high-latitudes, upwells over the world ocean and returns to polar bottom water forming zones via the meridional current flowing essentially in the surface ocean) was proposed by *Wyrtki* [1961] at least 30 years ago and has roots in physical oceanography going back considerably before that time. Air-sea exchange is modeled by an air sea exchange coefficient in combination with the buffer factor ξ that summarizes the chemical reequilibration of seawater in response to CO_2 variations. The buffer factor is calculated from the set of equations for borate, silicate, phosphate, and carbonate equilibrium chemistry and the temperature-dependent equilibrium constants as given by *Peng et al.* [1987]. An additional carbon source term is added to the deep ocean model to account for the oxidation of particulate organic carbon (POC). The sink of carbon due to new production of POC and the source of carbon due to particulate oxidation at intermediate depths contribute to a 5-10% lower concentration of ΣCO_2 in the surface waters compared to the deep waters. The observed range of the particulate fluxes is quite broad, ranging from 2 to 20 Gt C/yr [*Sundquist*, 1985; *Siegenthaler and Sarmiento*, 1993]. Flux calculations based on models, of course, depend inherently on model structure and assumptions. The marine biogenic flux of carbon in our model is 8.5 Gt C/yr which lies at the middle of the observed range.

The bottom water formation in the higher-latitude belts is quite well known [*Broecker and Peng*, 1982]. Most of the deep bottom water forms in the Weddell Sea in the southern hemisphere. In the UD model, the downwelling flow in a polar sea zone represents the bottom water forming regions of the world oceans. There is an important feedback for the atmospheric CO_2, namely, the direct interaction of atmospheric CO_2 with the deep ocean which is nearly free of excess CO_2. In the past, rapid vertical exchange between the polar surface waters and the deep ocean has been considered in several carbon cycle models [*Crane*, 1982; *Siegenthaler*, 1983; *Kheshgi et al.*, 1991]. In our model, bottom water concentration is controlled by newly introduced bottom water parameter π_c which is the change in the concentration of the bottom water N_b relative to that in the nonpolar region:

$$\pi_c = \frac{N_b - N_{b0}}{N_m - N_{m0}} \quad (1)$$

A value of $\pi_c = 1$ implies that the change in bottom water concentration is the same as the change in mixed layer concentration. However, other effects such as exposure of cold bottom water to the atmosphere could alter bottom water composition. The effect of uncertainties in this parameter can be quantified by using a range of values. When the model is run from 1765 to 1990 by specifying the atmospheric CO_2 concentration record, the model-estimated ocean uptake for the period 1980-1989 is 2.1± 0.1 Gt C/yr, for π_c = 0.5± 0.5. This is compared with the independent estimates [*Sarmiento and Sundquist*, 1992] of 2.0 ± 0.8 Gt C/yr for the same period. We use π_c=0.5 for total carbon and ^{14}C in our model results which follow. It is worth noting that the ratio of $^{14}C/^{12}C$ is insensitive to the value of π_c (the model-estimated change in the bomb ^{14}C inventories and penetration depth for the range of π_c =0.0-1.0 is <1%) and so measured ratios of $^{14}C/^{12}C$ cannot be used to choose the parameter π_c.

To estimate terrestrial biospheric fluxes, a six-box globally aggregated terrestrial biosphere submodel is coupled to the atmosphere box. The six boxes represent ground vegetation, nonwoody tree parts, woody tree parts, detritus, mobile soil (turnover time 70 years), and resistant soil (turnover time 500 years). The mass of carbon contained in the different reservoirs and the rate of exchange between them have been based on the analysis by *Harvey* [1989]. The model estimate of the global emission rate of CO_2 from changes in land use, from 1765 (preindustrial time) to 1990, is determined by the deconvolution of the atmospheric CO_2 concentration history (H.S. Kheshgi, et al., Accounting for the missing carbon sink with the CO_2 fertilization factor, submitted to *Climate Change*, 1994; hereinafter refereed to as Kheshgi et al., submitted manuscript, 1994). The model-estimated land use emissions are well within the error bounds (±1 Gt C/yr) of estimates of land use emissions summarized by *Schimel et al.* [1994].

The rate of photosynthesis by terrestrial biota is thought to be stimulated by increasing atmospheric carbon dioxide concentration. The increase in the rate of photosynthesis, relative to preindustrial times, is modeled to be proportional to the logarithm of the relative increase in atmospheric CO_2 concentration from its preindustrial value of 278 parts per million (ppm) [*Bacastow and Keeling*, 1973]. The proportionality constant β, known as the CO_2 fertilization factor, is chosen to be 0.42. The magnitude of the modeled biospheric sink is dependent on the chosen value of the CO_2 fertilization factor [*Harvey*, 1989; *Wigley*, 1993]. By varying the ambient CO_2 partial pressure for individual plants in controlled experiments under ideal growing conditions, a CO_2 fertilization effect has been demonstrated and found to lead to CO_2 fertilization factors ranging from 0.15 to 0.60 [*Kohlmaier et al.*, 1991]. Nutrient limitation and community competition for resources may, however, severely diminish ecosystem response to changing atmospheric CO_2 partial pressure [*Bazzaz and Fajer*, 1992]. The value of β = 0.42, however, is not prescribed by CO_2 fertilization experiments. The modeled magnitude of the CO_2 fertilization effect is chosen here to lead to a reconstruction of past carbon cycle, described by Kheshgi et al., submitted manuscript [1994], that matches the land use emission estimate [*Schimel et al.*, 1994] of 16.0 GtC for the decade 1980-1989. The rate coefficients for exchange to and from terrestrial biosphere boxes are temperature dependent according to an Arrhenius law.

In the appendix we describe the model equations for the ocean and atmosphere reservoirs of CO_2 and ^{14}C. These equations have been solved using a fourth-order Runga-Kutta method. A detailed description of various terrestrial components of the model is given by Kheshgi et al., submitted manuscript [1994].

Model Calibration to Preindustrial ^{14}C

There are two dynamic parameters in our model (the eddy diffusivity κ, and upwelling velocity w) which are calibrated by

matching the natural ^{14}C distribution in the deep ocean. Carbon 14 concentrations in this study are expressed as the deviations of $^{14}C/^{12}C$ ratio in parts per thousand (ppt) from the standard ratio that is expressed as $\Delta^{14}C$ [*Stuiver and Pollach*, 1977]. For the model calculations we use an arbitrary scale for $^{14}C/^{12}C$ ratio such that the preindustrial atmospheric ^{14}C ratio is 1 unit. When presenting the model results, we convert our arbitrary units into standard $\Delta^{14}C$ units as follows:

$$\Delta\,^{14}C = (\text{model units-1}) \times 10^3 \quad (2)$$

Therefore, in the preindustrial atmosphere, $\Delta^{14}C$ was equal to 0‰.

In the steady state, the rate of changes in atmosphere, mixed layer, and deep ocean concentrations are zero. Therefore the ocean ^{14}C ratio can be calculated by fixing the surface ocean and the polar sea values of total inorganic carbon and ^{14}C ratio. The preindustrial DIC concentrations in the mixed layer and the polar boxes of 2.03 mol/m^3 and the ^{14}C ratios in the corresponding boxes of 0.95 (-50‰) and 0.85 (-150‰) were estimated by *Broecker et al.* [1985] and *Broecker* [1963] and are used here to generate our initial conditions. The bomb-produced ^{14}C did not penetrate below the thermocline at the time of GEOSECS survey. Therefore the vertical profile of preindustrial ^{14}C ratio below 1000 m is well approximated by the global-average values estimated by *Shaffer and Sarmiento* [1994] from GEOSECS data. The values of κ and w required to match the preindustrial, vertical profile of ^{14}C are 4700 m^2/yr and 3.5 m/yr. The observed vertical profile of DIC for the oceans has also been estimated from the GEOSECS data by *Takahashi et al.* [1981]. The model estimated deep ocean profiles for ^{14}C concentration and total inorganic carbon are compared in Figures 2 and 3 with the GEOSECS-derived data. The $\Delta^{14}C$ value decreases across the main thermohaline, reaching a minimum of about -190‰ at a depth of 2.5 km; below this depth it rises again reaching the value of -178‰ at the ocean floor. The model-estimated mean ^{14}C ratio of -164‰ is in good agreement with the estimated global average value of -160‰ [*Oeschger et al.*, 1975]. The steady state concentration of DIC increases as one descends from the surface to reach a maximum and then decreases toward the ocean floor. The model-estimated mean DIC concentration of 2.30 mol/m^3 is close to the GEOSECS-derived value of 2.31 mol/m^3 [*Takahashi et al.*, 1981].

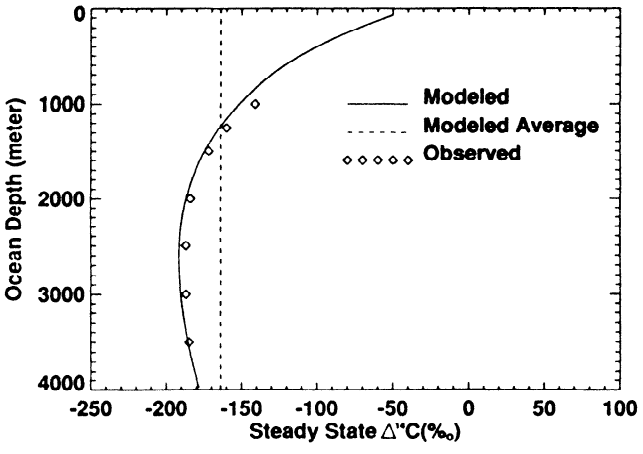

Figure 2. Comparison of the model simulated steady state ^{14}C (in per mil) in the ocean with the observed data. The estimated observed global mean values are taken from *Shaffer and Sarmiento* [1994].

The gas exchange flux was estimated (for the values of κ and w calibrated to match deep ocean ^{14}C) from the ^{14}C ratio of the surface reservoirs. The resulting global mean gas exchange rate at preindustrial CO_2 concentration of 278 ppm is 17.8 mol m^{-2} yr^{-1}, in close agreement with the *Sarmiento et al.*'s [1992] estimated gas exchange rate values 17.9 mol m^{-2} yr^{-1} at 275 ppm and with the value of 17.5 mol m^{-2} yr^{-1} at 280 ppm obtained by *Broecker et al.* [1985] from observed data. The bomb radiocarbon study of *Toggweiler et al.* [1989b] used a slightly lower value of the gas exchange rate of 16.6 mol m^{-2} yr^{-1}. Our flux value is also higher than the value of 15.2 mol m^{-2} yr^{-1} obtained by *Siegenthaler and Joos* [1992]. The difference in values could be due to the fact that we have used the actual profile of total inorganic carbon in the deep ocean, while *Siegenthaler and Joos* [1992] assumed constant concentration profile for the whole ocean equal to the surface ocean value, which is about 10% less than the mean ocean value.

Suess Effect

Fossil fuels are depleted of ^{14}C. The input of CO_2 from these sources lowers the atmospheric ratio of ^{14}C to total C by dilution. This effect was first determined by *Suess* [1955]. On the other hand, forest and soil carbon have ^{14}C ratio nearly the same as the atmospheric ratio; hence input or exchange of CO_2 from these sources has little effect on the atmospheric ^{14}C ratio if atmospheric ^{14}C is not changing. *Stuiver and Quay* [1980] suggest that changes in atmospheric ^{14}C could also be caused by changes in the production rate of ^{14}C which are correlated to the sunspot index. However, because of the uncertainty in the variation of production rate of ^{14}C and its negligible effect on ^{14}C ratio [*Bacastow and Keeling*, 1973] over the timescale of the Suess effect, we do not account for this effect in our calculation and thus assume constant ^{14}C production. The Suess effect is apparent in measured atmospheric ^{14}C before the 1950s, at which time the ^{14}C ratio increased drastically due to emissions from nuclear bomb detonations. High-precision tree ring measurements of atmospheric ^{14}C levels between 1840 and 1950 show a decrease of about 24‰ as shown in Figure 4 [*Stuiver and Quay*, 1981]. In another analysis of tree ring data, *Keeling* [1973] found a slightly higher Suess effect of -25‰ over the same time period.

Carbon cycle models have been used to predict the size of the atmospheric Suess effect up to 1950. *Bacastow and Keeling* [1973] estimated a Suess effect of about -23 ± 4‰ using their one-dimensional (1-D) model, while *Oeschger et al.* [1975] estimated a value of -20‰. Our UD model estimates an atmospheric ^{14}C change of -25‰. In Figure 4, the Suess effect estimated by our UD model over the time period from 1840 to 1950 is seen to be consistent with tree ring data.

The surface ocean also shows a Suess effect. *Druffel and Linick* [1978] and *Druffel and Suess* [1983] measured a change of -9 ± 3‰ in the surface ocean ^{14}C ratios over the period 1850-1950. This estimate is based on the average of the radiocarbon measurements for the Pacific and the Atlantic corals which

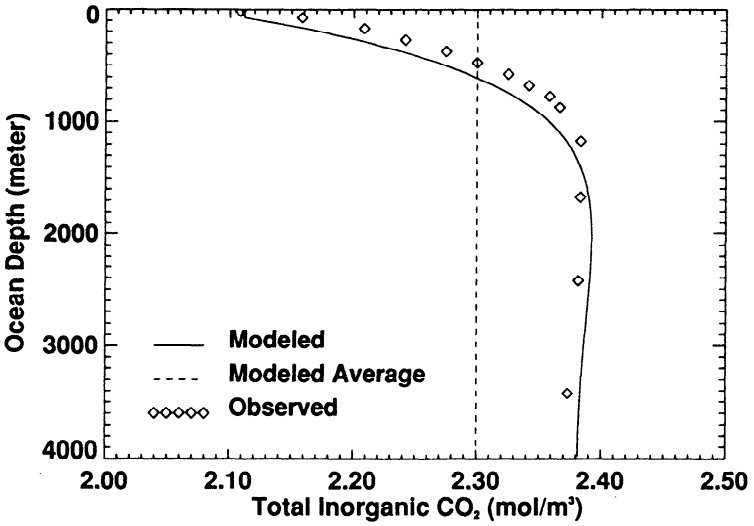

Figure 3. Comparison of the model estimated total inorganic carbon (in moles per cubic meter) in 1974 with observed ocean data. The observed data are a global average of the GEOSECS data which were taken over the period 1972-1978 [*Takahashi et al.*, 1981].

includes, for example, Florida coral (-11‰), Belize coral (-12‰), and Galapagos coral (-6‰). The UD model predicts a mixed layer Suess effect of -9‰ over the same period, again consistent with observations.

Bomb Produced ^{14}C

Bomb tests carried out during the period 1954-1963 produced about 700 x 10^{26} ^{14}C atoms [*Broecker and Peng*, 1982]. The bomb ^{14}C tracer interrogates mixing processes capable of removing ^{14}C (or CO_2) from the atmosphere on the decade timescale. It has been hypothesized [*Broecker et al.*, 1980] that models capable of predicting bomb ^{14}C distributions will also be capable of predicting the uptake of anthropogenic CO_2 which also has a similar characteristic timescale (≈ 20 years). This is in contrast to the preindustrial distribution of ^{14}C, which was used to calibrate the ocean mixing parameters κ and w, and is sensitive to slow mixing processes (≈ 500 years) approaching the half-life time of radiocarbon (5730 years). It is therefore important to check whether our model can also reproduce the measured distribution of the bomb ^{14}C. This check tests whether the ratio of air-sea exchange to vertical mixing resistance just beneath the mixed layer is of the right magnitude. Since the production data of ^{14}C produced by nuclear weapons tests are not precisely known, the average observed atmospheric concentrations, shown in Figure 5, are prescribed from 1950 to 1975 in order to estimate the uptake of bomb ^{14}C by the ocean. Figure 6 shows the observed- and model-estimated ^{14}C distributions in the ocean for the year 1974 which clearly show the effects of bomb-produced ^{14}C. The observed values were derived from GEOSECS data by *Shaffer and Sarmiento* [1994]. Although the model slightly underestimates the bomb ^{14}C concentration in the upper ocean, elsewhere the model is able to reproduced the observed bomb ^{14}C distribution.

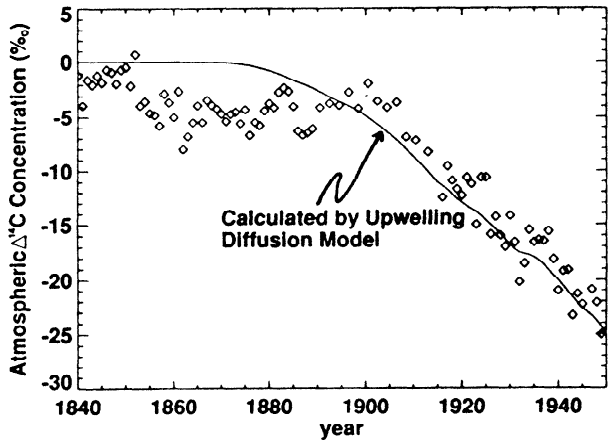

Figure 4. Comparison of the model estimated atmospheric ^{14}C decrease caused by the dilution of ^{14}C by fossil fuel CO_2 (i.e., the Suess effect) with the tree rings measurements of *Stuiver and Quay* [1981] from 1840 to 1950.

The observed mean concentration of bomb ^{14}C in surface water, defined as the difference between the postbomb $\Delta^{14}C$ and the prebomb $\Delta^{14}C$, was 160±15‰ [*Broecker et al.*, 1985]. The UD model predicts 172‰ for the period 1950-1974 which lies within the limit of uncertainties.

The average oceanic inventory of bomb ^{14}C ($\Sigma^{14}C$) defined as the excess ^{14}C amount over the prebomb level, is determined [*Broecker et al.*, 1985] by integrating the difference between the prebomb and postbomb vertical profiles as

$$\Sigma^{14}C = \int_0^{4000m} \left[\Sigma CO_2(\Delta^{14}C - \Delta^{14}C_{1950})\right] dz \qquad (3)$$

where $\Delta^{14}C_{1950}$ and $\Delta^{14}C$ are the pre and post-bomb ocean surface concentration and ΣCO_2 is the DIC concentration. The penetration depth Z is

$$Z = \int_0^{4000m} (\Delta^{14}C - \Delta^{14}C_{1950}) dz \Big/ (\Delta^{14}C - \Delta^{14}C_{1950})\Big|_{z=0} \qquad (4)$$

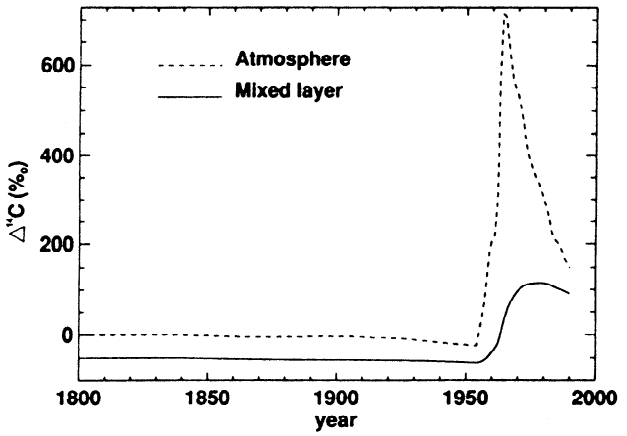

Figure 5. Model estimated ^{14}C concentration (per mil) in mixed layer from 1800 to 1990. The atmospheric ^{14}C concentration changes until 1950, due to dilution by fossil fuel CO_2, are calculated with the carbon cycle model. Thereafter, concentrations are prescribed according to observation [*Tans*, 1981].

An ocean average model-estimated DIC concentration of 2.1 mol/m^3 is used for ΣCO_2 when evaluating (3) and (4). The model-estimated bomb CO_2 inventories and penetration depths from 1955 to 1975 are shown in Figures 7 and 8. For 1974 (time of the GEOSECS survey) the model-estimated bomb ^{14}C inventory and the penetration depth are 8.3 x 10^{13} atoms/m^2 and 308 m, respectively. From the GEOSECS data, *Broecker et al.* [1985] estimated the total-ocean inventory to be about 2.9x10^{28} atoms. If we divide this value by the world's ocean area (3.6 x 10^{14} m^2), the average bomb ^{14}C inventory is 8.0±0.5 x 10^{13} atoms/m^2 and the resulting penetration depth is 328±20 m. Our model-estimated value for bomb ^{14}C inventory is about 4% higher as compared to observed data, whereas the estimated penetration depth is about 7% lower. There could be two reasons for these minor differences. First, the total CO_2 concentration value used in our calculation is higher than the value of 2.15 mol/m^3 [*Toggweiler et al.*, 1989b] used by *Broecker et al.*

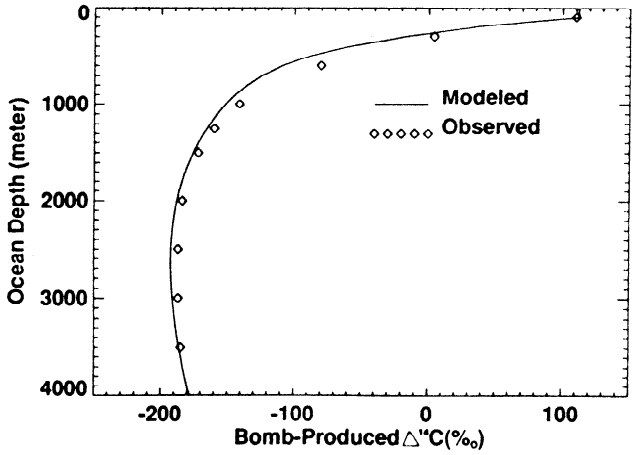

Figure 6. Comparison of the model-estimated bomb-produced ^{14}C (in per mil) in the deep ocean with the observed data. The observed values, estimated from the GEOSECS data, are taken from *Shaffer and Sarmiento* [1994].

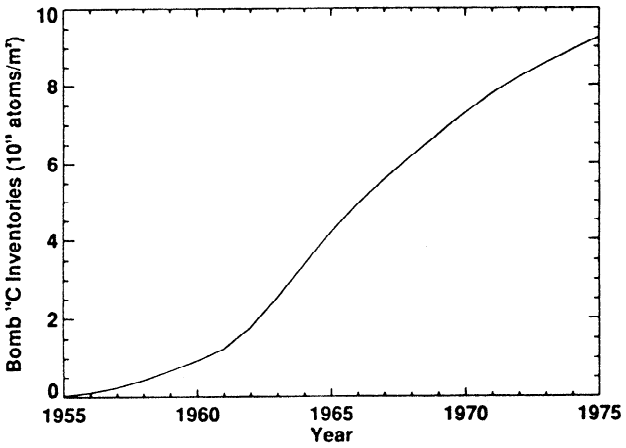

Figure 7. Model-estimated vertically integrated inventories of bomb ^{14}C (10^{13} atoms/m^2) from 1955 to 1975.

[1985]. Second, the prenuclear (1950) surface water concentration in our calculations is lower (-59‰) than that (-50‰) used by *Broecker et al.* [1985]. This is due to the fact that we start the calculation from preindustrial time with prescribed biospheric and fossil emissions, which results in a Suess effect of -25‰ in surface water, while *Broecker et al.* [1985] start the calculations in 1950 with the preindustrial atmospheric and ocean ^{14}C ratios and ΣCO_2.

Model Intercomparison

The results of the UD model are also compared in Table 2 with those of a pure diffusion model [*Siegenthaler*, 1983], high-latitude exchange/interior diffusion advection (HILDA) [*Siegenthaler and Joos*, 1992], and ocean general circulation models (OGCMs) [*Toggweiler et al.*, 1989b; and M. Heimann, personal communication, 1993].

Many of the simple models have been calibrated using the distribution of ^{14}C tracer. *Siegenthaler* [1983] calibrated their model parameters by means of the postbomb ^{14}C distribution in the deep sea; however, the estimated mean deep ocean value for

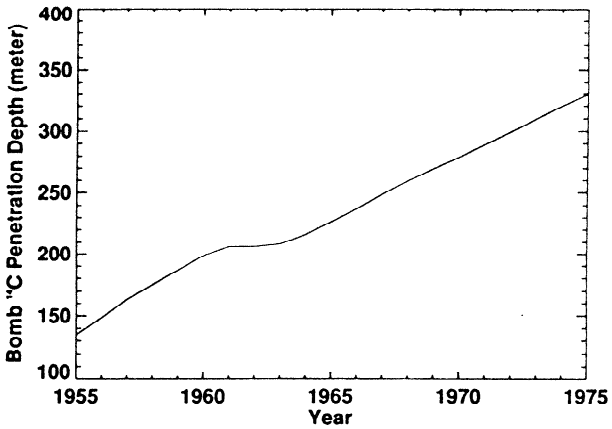

Figure 8. Model-estimated mean penetration depth (in meters) for excess ^{14}C from 1955 to 1975.

the preindustrial time was about 30% higher than the observed values (Table 2). Using the HILDA model, *Siegenthaler and Joos* [1992] found that to produce natural as well as bomb ^{14}C distribution in the ocean, the vertical diffusivity κ in their model must be reduced with depth. In contrast, the UD model is able to reproduce both the natural and bomb ^{14}C distribution in ocean with the constant diffusivity, as indicated in previous sections. It should be noted that the structure of the UD model differs from the HILDA model in that the HILDA model requires, in addition to upwelling velocity (w) and diffusivity (κ), two more tunable parameters: water exchange between the high-latitude surface and deep ocean boxes (u), and between the high- and low-latitude deep ocean boxes (q). Also, the upwelling velocity used in the HILDA model is very small (w = 0.7 m/yr) as compared to our value (w = 3.5 m/yr). Our higher value is in closer agreement with the upwelling velocity derived from ocean overturning rates (w = 4 m/yr) [*Gordon and Taylor*, 1975]. It must also be pointed out that contrary to *Siegenthaler and Joos* [1992], we also take into account the downward transport of ^{14}C by the rain of organic particles produced by marine organisms. Neglecting this biological effect can introduce errors up to 10% in the steady state profile of ^{14}C ratios [*Fiadeiro*, 1982]. Even so, Table 2 shows that the changes predicted by the HILDA and UD models are quite close to the observed values.

Table 2 also shows that the results of the two OGCMs presented do not lie within the range of uncertainty of the observed data, as did the UD results. The *Toggweiler et al.* [1989b] results are determined from the Geophysical Fluid Dynamics Laboratory (GFDL) primitive equation OGCM [*Bryan*, 1987]. M. Heimann's (personal communication, 1993) results are based on the Hamburg Large Scale Geostrophic OGCM [*Maier-Reimer et al.*, 1993]. While the GFDL model predicts a mean

Table 2. Comparison of Upwelling-Diffusion Model (UD) Results with Observations and Other Different Model Results

					OGCM	
	Observation	UD Model, This Study	HILDA Model, *Siegenthaler and Joos* [1992][a]	Diffusion Model, *Siegenthaler* [1983]	*Toggweiler et al.*[1989a,b][b]	M. Heimann, (personal communication, 1994)
Preindustrial (1765) ocean surface $\Delta^{14}C$ ‰	-49 ± 3[c]	−50	−55	−46	—	—
Prebomb (1950) ocean surface $\Delta^{14}C$ ‰	-58 ± 3[c]	−59	−62	−53	−50	—
Bomb $\Delta^{14}C$ in ocean surface ‰[d]	160 ± 15[e]	171	155	163	160	206
Mean ^{14}C for the deep-sea $\Delta^{14}C$, ‰	−160[f]	−163	—	−110	—	—
Total CO_2 concentration ΣC, mol/m^3[g]	2.15[h]	2.18	2.13	2.05	2.15	—
Bomb ^{14}C inventories, 10^{13} atoms/m^2	8.00 ± 0.5[e]	8.30	7.95	8.42	6.90	9.27
Penetration depth, m	328 ± 20[i]	308	338	355	283	320
Oceanic CO_2 uptake, 1980s, Gt C/yr	2.0 ± 0.8[j]	2.10	2.15	3.33	1.67	1.45

a) Values for HILDA model are area weighted mean from low- and high-latitude belts.

b) Assume prebomb atmosphere(1950) in steady state atmosphere.

c) Estimates are based on the Pacific and Atlantic corals [*Druffel and Suess*, 1983].

d) Defined as the difference between the $\Delta^{14}C$ at the time of GEOSECS and the prebomb $\Delta^{14}C$.

e) *Broecker et al.* [1985].

f) Weighted mean of Atlantic and Pacific data [*Oeschger et al.*, 1975].

g) Average value for that part of the water column which is contaminated with bomb ^{14}C.

h) Estimated by *Toggweiler et al.* [1989a,b] from the GEOSECS observations.

i) Estimated from the formula of *Broecker et al.* [1985].

j) Estimate [*Sarmiento and Sundquist*, 1992] of ocean carbon uptake based on measurements outlined by *Tans et al.* [1990].

surface water bomb ^{14}C concentration of 160‰, in agreement with the GEOSECS record, the prediction of the bomb ^{14}C inventory and penetration depth are too low as compared to the observations. On the other hand, the Hamburg model predicts very high values of bomb ^{14}C surface concentrations, about 23% higher than the observed value. The bomb ^{14}C inventory is higher by about 16% than the observed value, even though it does reproduce the observed bomb ^{14}C inventory. These results suggest that the current published OGCMs do not correctly simulate the atmospheric-ocean exchange and the vertical mixing in the upper ocean. Therefore such models in their current state should not be used to predict either current or future uptake of CO_2 by the oceans.

The models listed in Table 2 yield an ocean CO_2 uptake rate for the 1980s of between 1.45 and 3.33 Gt C/yr. Both GCMs [*Toggweiler et al.*, 1989a; *Maier-Reimer et al.*, 1993] underpredict the ocean CO_2 uptake rate, while the diffusion model [*Siegenthaler*, 1983] overpredicts the ocean CO_2 uptake. The UD model and the HILDA model results lie near the center of the uncertainty band of *Sarmiento and Sundquist's* [1992] estimate for the current ocean uptake of 2.0± 0.8 Gt C/yr.

Radiocarbon Estimates of Terrestrial Biosphere

The magnitude and the timing of the terrestrial ecosystems response to changes in the land use and climate are a large source of uncertainty in global carbon cycle models. An understanding of these uncertainties requires knowledge of both the inventory of carbon in the biosphere (including soils) and the turnover rate of carbon in the carbon reservoirs, in particular, the soil reservoir. An estimated 1300 to 1500 Gt C are stored globally as organic matter in the upper meter of mineral soils [*Schlesinger*, 1991] which is roughly twice the estimated storage of carbon in atmosphere or in the living biosphere [*Houghton et al.*, 1990]. Attempts have been made to model the turnover times of soil carbon reservoirs with the aid of soil ^{14}C measurements [*Harrison et al.*, 1993; *Trumbore*, 1993]. In this paper, however, we do not attempt to estimate the soil carbon turnover rates from ^{14}C data, realizing that there are not only the uncertainties in the observed data but also in the soil carbon dynamics [*Stevenson and Elliott*, 1990]. Instead, we use the turnover times reported by *Harvey* [1989].

To estimate the terrestrial biospheric uptake of radiocarbon, we use a six-reservoir terrestrial model, as shown in Figure 1. Turnover times for the terrestrial reservoirs range from approximately 1 year for nonwoody tree parts to 20 years for woody tree parts and 70 and 500 years for mobile (fast cycling) and resistant (slow cycling) soil reservoirs (Table 3). We assume a fertilization factor ß =0.42. We also take into account a temperature-respiration feedback in our calculations. However, the global mean temperature over the time period considered here is too small to lead to an appreciable change in the modeled respiration rates. In steady state the model-estimated ^{14}C concentrations of terrestrial reservoirs are -36‰ for ground vegetation, -36‰ for nonwoody tree parts, -38‰ for woody tree parts, -37‰ for detritus, -45‰ for mobile soil, and -96‰ for resistant soil (see Table 3). Changes in atmospheric ^{14}C concentrations have an impact first on terrestrial carbon reservoirs with short turnover times and have little influence on terrestrial carbon reservoirs with long turnover times. We have studied two ^{14}C effects: ^{14}C dilution (Suess effect), and ^{14}C enhancement (bomb-produced). The model estimated dilution of atmospheric ^{14}C caused by fossil fuel CO_2 from 1765 to 1950 was about -25 ‰ (Table 3) and the observed ^{14}C increase due to nuclear bomb tests from 1950 to 1964 was about +737 ‰. In 1964, nuclear tests were banned and since then the atmospheric ^{14}C concentration has decreased exponentially (Figure 5). The carbon reservoir having a shortest turnover time, 0.7 years, follows the atmospheric signal; ^{14}C concentration reduction for this reservoir is 20‰ from 1765 to 1950 and increase is 622‰ from 1950 to 1964 (Table 3). In contrast, the carbon reservoir

Table 3. Turnover Times and ^{14}C Concentrations for Terrestrial Reservoirs for Preindustrial (1765), Prebomb (1950), and Postbomb (1964) Years

Reservoir	Turnover Time, years	^{14}C Concentration, ‰				
		1765	1950	1964	1950-1765	1964-1950
Atmosphere		0	-25	712	-25	737
Ground vegetation	2.0	-36	-56	398	-20	454
Nonwoody tree parts	0.7	-36	-56	566	-20	622
Woody tree parts	20.0	-38	-53	23	-15	76
Detritus	1.8	-37	-55	227	-18	82
Mobile soil	70.0	-45	-51	-43	-6	8
Resistant soil	500.0	-96	-96	-95	0	1

Also given are the ^{14}C concentration differences for the prebomb and preindustrial time period (1950-1765) and post and prebomb time period (1964-1950).

having longest turnover time, 500 years, shows the least changes. The resistant soil reservoir experiences almost no appreciable change from 1765 to 1950 and only 1‰ increase from 1950 to 1964 (Table 3).

The global terrestrial biospheric uptake of bomb radiocarbon can not be compared with observations, because there are no observational estimates available in the literature. However, we have compared our model results with other recently published model estimates. *Joos* [1994] has estimated the terrestrial biospheric bomb radiocarbon inventories for the period 1965 to 1989 to be $75 \pm 30 \times 10^{26}$ atoms. This estimate is simply based on the average of four carbon cycle model results. The individual estimates of four models are 60×10^{26} [*Hesshaimer et al.*, 1994], 45×10^{26} [*Broecker et al.*, 1985], 89×10^{26} [*Siegenthaler and Oeschger*, 1987], and 99×10^{26} atoms [*Siegenthaler and Joos*, 1992], respectively. Our model estimated bomb radiocarbon inventory for the terrestrial biosphere reservoir for the same period (1965-1989) is 80×10^{26} atoms which is well within the range of *Joos'* [1994] estimates.

Temperature Change

We now examine whether the model dynamic parameters κ and w that are derived from the ^{14}C calibration are able to simulate vertical temperature distribution. Figure 9 shows that the UD model does not accurately reproduce the *Levitus* [1982] horizontal average distribution of potential temperature in the deep ocean. The results from the prognostic OGCM [*Toggweiler et al.*, 1989a] and HILDA [*Siegenthaler and Joos*, 1992] models are also shown in Figure 9. The HILDA model yields temperatures that are too high overall. The results found by both our UD model and by *Toggweiler et al.* [1989a] in their OGCM are remarkably similar. We find that both models give temperatures near the thermocline which are too warm, although the bottom water and mixed layer temperatures are in agreement with observations. It seems that the apparent upper ocean diffusivity for the uptake of the bomb radiocarbon is considerably more intense than that needed to match the steady state vertical temperature profile. This is consistent with the hypothesis that tracers, such as ^{14}C, with concentration contours crossing isopycnal contours will see enhanced vertical mixing relative to temperature which has isotherms virtually parallel to isopycnals. Therefore we reach a conclusion similar to that of *Siegenthaler and Joos* [1992] in that the UD model is not able to predict the distribution of both temperature and ^{14}C with one set of dynamic parameters.

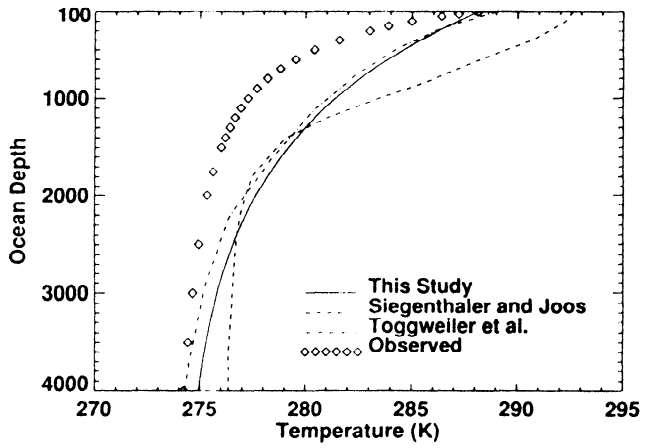

Figure 9. Comparison of the depth dependence of equilibrium mean deep ocean temperature compared between observations [*Levitus*, 1982], this model result, OGCM carbon cycle model results [*Toggweiler et al.*, 1989a], and a HILDA model result [*Siegenthaler and Joos*, 1992].

Concluding Discussion

A carbon cycle model describing the exchange of carbon among the atmosphere, ocean, and terrestrial biosphere is found to be consistent with measured values (within measurement error) of the prebomb rise in ^{14}C in the atmosphere and the mixed layer due to the Suess effect, the bomb ^{14}C in the mixed layer, the bomb ^{14}C penetration depth, the bomb ^{14}C ocean inventory, and the vertical distribution of total carbon. This is the first study to recognize that a simple upwelling-diffusion model for the deep ocean can reproduce all of these features by calibration of only two parameters, κ and w. The thermocline depth scale κ/w = 1343 m found by calibration to steady state ^{14}C is considerably deeper than that required to match the steady vertical temperature profile (500 m); this is consistent with the hypothesis that isopycnal mixing, which is much more rapid than diapycnal mixing, has a stronger effect on ^{14}C than on temperature since isopycnals are nearly isothermal [*Hoffert and Flannery*, 1985]. Results are compared to those of one other schematic carbon cycle model as well as those of two ocean general circulation models which have also attempted to reproduce the ^{14}C records. The GCMs' results lie outside the range of uncertainties of the records, while the schematic model (HILDA) proposed by *Siegenthaler and Joos* [1992] succeeded. The HILDA model, however, required the use of an extremely low upwelling velocity as well as a vertical eddy diffusivity that decreases with depth in contradiction to our understanding of bottom water formation and ocean mixing [*Gordon and Taylor*, 1975; *Gargett and Holloway*, 1984]. The UD and HILDA models use different approximations to represent the effects of bottom water formation and rapid mixing in the high-latitude oceans.

We introduce the parameter π_C, which is the change in the concentration of the bottom water relative to that in the mixed layer. Model ^{14}C results are not sensitive to this parameter, although the ultimate response of the system to emissions is sensitive to π_C. We choose the value of $\pi_C = 0.5$ from independent estimates of ocean carbon uptake. Thus calibrated, this model for the global carbon cycle is intended for use in predicting the rise of atmospheric CO_2 due to emissions; future studies will address such analyses.

Appendix

The rate of change of carbon in the model atmosphere is governed by

$$\frac{dN_a}{dt} = k_a\left(\frac{N_{ao}}{N_{mo}}\right)(N_{mo} + \xi n_m) - k_a n_a + F_e + B_e \qquad \text{(A1)}$$

where the mass of carbon (in gigatons carbon) in the atmosphere is $N_a = N_{ao} + n_a$ and $N_{ao} = 590$ Gt C is the preindustrial atmospheric carbon mass. The mass of dissolved inorganic carbon (Gt C) in the mixed layer is $N_m = N_{mo} + n_m$ and $N_{mo} = 676$ Gt C is the preindustrial mixed layer carbon mass. The atmospheric rate of exchange is $k_a = 0.11$ yr^{-1}. The mass rate of fossil fuel emissions to the atmosphere is F_e. The net terrestrial mass rate of emissions to the atmosphere is B_e. The buffering action of seawater is taken into account by multiplying the excess CO_2 content of the mixed layer (n_m) by buffer factor ξ, where

$$\xi = \frac{(P_m - P_{m0})/P_{m0}}{(N_m - N_{m0})/N_{m0}} \tag{A2}$$

P_m is the equilibrium CO_2 partial pressure of seawater in the mixed layer, and $P_{m\,0} = 769.79$ μatm is preindustrial value. Partial pressure P_m is calculated from the set of chemical equilibrium equations for borate (Tb), silicate (Tsi), phosphate (Tp), total alkalinity (Talk), silicate (*s*), and carbonate. Concentrations Tb, Tsi, Tp, Talk, and *s* are assumed to remain constant in the mixed layer. Following *Peng et al.* [1987] these concentrations are taken to be Tb=409.07 μ*M* kg^{-1}, Tsi=46.5 μ*M* kg^{-1}, Tp=1.43 μ*M* kg^{-1}, Talk=2333 μ*M* kg^{-1}, and s=34.26‰, respectively.

The rate of change of carbon in the model mixed layer is governed by

$$\frac{dN_m}{dt} = -k_a\left(\frac{N_{ao}}{N_{mo}}\right)(N_{mo} + \xi n_m) + k_a N_a + A\Omega\kappa\left.\frac{\partial N_d}{\partial z}\right|_{z=0} + A\Omega w[N_d(0) - N_b] - F_g \tag{A3}$$

where the surface area of the oceans is $A = 3.62 \times 10^{12}$ m^2. The vertical eddy diffusivity in the deep ocean column $\kappa = 4700$ m^2/yr and upwelling velocity $w = 3.5$ m/yr are model parameters calibrated by matching the depth variation of preindustrial ^{14}C. The conversion factor $\Omega = 1.2 \times 10^{-14}$ Gt C/mol C. In the above equations, F_g is the net marine biogenic flux of carbon leaving the mixed layer, i.e., the new production, and is taken to be 8.5 Gt C/yr [*Bacastow and Maier-Reimer*, 1991; *Najjar et al.*, 1992].

The rate of change of carbon in the model deep ocean column is governed by

$$\frac{\partial N_d}{\partial t} = \kappa\frac{\partial^2 N_d}{\partial^2 z} + w\frac{\partial N_d}{\partial z} + J \tag{A4}$$

where N_d is the concentration of dissolved inorganic carbon (in moles C per cubic meter) and J is the source of carbon by from respiration of particulate organic carbon. The strength of the source $J(z)$ is assumed to decrease exponentially with depth with an exponential depth scale of 750 m [*Volk and Hoffert*, 1985], which roughly matches the scattered data on organic particulate flux derived from sediment trap measurements which best fits a profile proportional to $1/z$ [*Berger et al.*, 1987]. This partial differential equation has the boundary conditions

$$N_d = \frac{N_m}{A\Omega h_m} \qquad \text{at } z = h_m \tag{A5}$$

$$\kappa\frac{\partial N_d}{\partial z} + wN_d = wN_b \qquad \text{at } z = h_d \tag{A6}$$

where $h_d = 4{,}000$ m is the mean depth of the ocean and $h_m = 75$ m is the mean depth of the mixed layer. The bottom water concentration N_b is determined by (1). The depth below the mixed layer is z.

The amount of ^{14}C is given by the product of carbon mass or concentration N and the ^{14}C ratio R. The equation for the mass balance of atmospheric ^{14}C is

$$\frac{dN_aR_a}{dt} = k_a\left(\frac{N_{ao}}{N_{mo}}\right)(N_{mo} + \xi n_m)\alpha_{ma}R_m - k_aN_a\alpha_{am}R_a + \bar{Q}_p + B_{er} - \lambda N_aR_a \tag{A7}$$

where R_a, R_m and R_b are the mole ratios of ^{14}C to carbon in the atmosphere, mixed layer, and terrestrial biospheric emissions. Preindustrial values for R_a and R_m are 0‰ and -50‰. Here α_{am} and α_{ma}, are the ^{14}C fractionation factors for CO_2 uptake by the surface ocean and CO_2 evasion from the surface ocean. The factors α_{am} and α_{ma}, according to *Keeling* [1973], are 0.972, and 0.955. Note that no term appears for fossil fuel emissions since fossil fuels are depleted in ^{14}C. The decay constant λ of ^{14}C is 1/(8267 years). The mean production rate $\bar{Q}_p$ of ^{14}C from cosmic ray flux is taken to be equal to 2 atom cm^{-2} s-1. The transfer of ^{14}C from the terrestrial biosphere to the atmosphere is B_{er}, where

$$B_{er} = R_a\alpha_{ab}(-F_{at,gv} - F_{at,nw}) + \sum_{i=1}^{6}(R_{bi}F_{i,at} + R_{bi}Flu_i) \tag{A8}$$

and where R_{bi} is the ^{14}C ratio of the ith terrestrial reservoir. The preindustrial values of R_{bi} are given in Table 3. Flu_i is the net land use emission contribution of the ith biosphere reservoir. $F_{i,at}$ is the flow of carbon from terrestrial reservoir i to atmosphere. Similarly, $F_{at,gv}$ and $F_{at,nw}$ are the carbon flows from the atmosphere reservoir to the ground vegetation and nonwoody tree reservoirs. The steady state values of $F_{i,at}$ and $F_{at,i}$ are given by *Harvey* [1989]; α_{ab} is the $^{14}C/^{12}C$ fractionation factor for CO_2 uptake by the terrestrial biosphere which is approximately square of that for $^{13}C/^{12}C$. According to *Keeling et al.* [1989a] the fractionation factor for $^{13}C/^{12}C$ is 0.982, and hence for $^{14}C/^{12}C$, $\alpha_{ab} = 0.964$.

The equation for the mass balance of mixed layer ^{14}C is

$$\frac{dN_mR_m}{dt} = k_aN_a\alpha_{am}R_a - k_a\left(\frac{N_{ao}}{N_{mo}}\right)(N_{mo} + \xi n_m)\alpha_{ma}R_m - \lambda N_mR_m + A\Omega\kappa\left.\frac{\partial N_dR_d}{\partial z}\right|_{z=h_m} + A\Omega w[(N_dR_d)|_{z=h_m} - N_bR_b] - F_gF_g^* \tag{A9}$$

where R_d is the mole ratio of ^{14}C to carbon in the ocean column.

The equation for the mass balance of ocean column ^{14}C is

$$\frac{\partial N_d R_d}{\partial t} = \kappa \frac{\partial^2}{\partial^2 z}(N_d R_d) + w\frac{\partial}{\partial z}(N_d R_d) + J_d J_d^* - \lambda N_d R_d \quad \text{(A10)}$$

with boundary conditions

$$N_d R_d = \frac{N_m R_m}{A\Omega h_m} \qquad \text{at } z = h_m \quad \text{(A11)}$$

$$\kappa \frac{\partial}{\partial z}(N_d R_d) + w N_d R_d = w N_b R_b \qquad \text{at } z = h_d \quad \text{(A12)}$$

The magnitude of the marine biosphere carbon source and the sink terms are not affected by the addition of fossil fuel CO_2 to the oceans because the biological productivity, according to the present understanding, is primarily limited by the nutrients such as phosphate and nitrate, and not CO_2 [*Siegenthaler and Sarmiento*, 1993]. The biological flux in our model acts as a natural background process and does not change with time. The corresponding ratios F_g^* and J^* of ^{14}C, however, follow the time-varying mixed layer ratio R_m times a fractionation factor of 0.954 [*Toggweiler and Sarmiento*, 1985].

Acknowledgments. Work was performed under the auspices of the U.S. Department of Energy at the Lawrence Livermore National Laboratory under contract W-7405-Eng-48 and was supported in part by the Department of Energy's Environmental Science Division. We thank J. R. Toggweiler and M. Heimann for contributing their GCM results for comparison.

References

Bacastow, R., and C. D. Keeling, Atmospheric carbon dioxide and radiocarbon in the natural carbon cycle, II, Changes from A. D. 1700 to 2070 as deduced from a geochemical model, in *Carbon in the Biosphere, AEC Symp. Ser.*, vol. 30, edited by G. M. Woodwell, and E. V. Pecan, pp. 86-135, National Technical Information Service, U.S. Department of Commerce, Springfield, Va., 1973.

Bacastow, R., and E. Maier-Reimer, Ocean circulation model of the carbon cycle, *Clim. Dyn.*, *4*, 95-125, 1990.

Bacastow, R. B., and E. Maier-Reimer, Dissolved organic carbon in modeling oceanic new production, *Global Biogeochem. Cycles*, *5*, 71-85, 1991.

Bazzaz, F. A., and E. D. Fajer, Plant life in a CO_2-rich world, *Sci. Am.*, *264*, 68-74, 1992.

Berger, W. H., K. Fischer, C. Lai, and G. Wu, Ocean productivity and oceanic carbon flux, I, Overview and maps of primary production and export production, *SIO Ref. 87-30*, Scripps Inst. of Oceanogr., Univ. of Calif., San Diego, La Jolla, 1987.

Bjorkstrom, A., A model of CO_2 interaction between atmosphere, oceans, and land biota, in *The Global Carbon Cycle*, Scope 13, edited by B. Bolin et al., pp. 403-457, John Wiley, New York, 1979.

Bjorkstrom, A., One-dimensional and two-dimensional ocean models for predicting the distribution of CO_2 between the ocean and the atmosphere, in *The Changing Carbon Cycle*, edited by J.R. Trabalka and D.E. Reichle, pp. 258-278, Springer-Verlag, New York, 1986.

Boden, T.A., R.J. Sepanski, and F.W. Stoss, *Trends '91: A Compendium of Data on Global Change*, 665 p., Carbon Dioxide Information Analysis Center, Oak Ridge National Laboratory, Oak Ridge, Tenn., 1991.

Bolin, B., and E. Eriksson, Changes in the carbon content of the atmosphere and sea due to fossil fuel combustion, in *The Atmosphere and Sea in Motion*, edited by B. Bolin, Rockefeller Institute Press, New York, 1959.

Bretherton, F.P., K. Bryan, and J.D. Woods, Time-dependent greenhouse-gas-induced climate change, in *Climate Change: The IPCC Assessment*, edited by J.T. Houghton et al., pp. 173-193, Cambridge University Press, New York, 1990.

Broecker, W. S., Radioisotopes and large-scale oceanic mixing, in *The Sea*, vol. 2, edited by N.M. Hill, pp. 88-108, Wiley-Interscience, New York, 1963.

Broecker, W.S., and T.-H. Peng, *Tracers in the Sea*. 691 p., Lamont-Doherty Earth Observatory, Palisades, N.Y., 1982.

Broecker, W.S., and T.H. Peng, Carbon cycle 1985, glacial to interglacial changes in the operation of the global carbon cycle, *Radiocarbon*, *28*(2A), 309-327, 1986.

Broecker, W.S., and T.-H. Peng, The role of $CaCO_3$ compensation in the glacial to interglacial atmospheric CO_2 change, *Global Biogeochem. Cycles*, *1*, 15-39, 1987.

Broecker, W.S., Y.-H. Li, and T.-H. Peng, Carbon dioxide – man's unseen artifact, in *Impingment of Man on the Oceans*, edited by D.W. Hood, pp. 287-324, Wiley-Interscience, New York, 1971.

Broecker, W. S., T.-H. Peng, and R. Eng, Modeling the carbon system, *Radiocarbon*, *22*, 565-580, 1980.

Broecker, W.S., T.-H. Peng, G. Ostlund, and M. Stuiver, The distribution of bomb radiocarbon in the ocean, *J. Geophys. Res.*, *90*, 6953-6970, 1985.

Bryan, F., Parameter sensitivity of primitive equation ocean general circulation models, *J. Phys. Oceanogr.*, *17*, 970-985, 1987.

Caldeira, K., M.I. Hoffert, and A.K. Jain, Simple ocean carbon cycle models, in *Proceeding of the 1993 Global Change Institute on the Carbon Cycle*, edited by T.M.L. Wigley, and D. Schimal, Cambridge University Press, in press, 1994.

Crane, A. J., The partitioning of excess CO_2 in a five-reservoir atmosphere-ocean model, *Tellus*, *34*, 398-405, 1982.

Druffel, E. M., and T.W. Linick, Radiocarbon in annual coral rings of Florida, *Geophys. Res. Lett.*, *5*, 913-916, 1978.

Druffel, E. M. and H.E. Suess, On the radiocarbon record in banded corals, *J. Geophys. Res.*, *88*, 1271-1280, 1983.

Fiadeiro, M. E., Three dimensional modeling of tracers in the deep pacific ocean, II, Radiocarbon and circulation, *J. Mar. Res.*, *40*, 537-550, 1982.

Gargett, A.E., and G. Holloway, Dissipation and diffusion by internal wave breaking, *J. Mar. Res.*, *42*, 15-27, 1984.

Gordon, A. L., and H.W. Taylor, Heat and salt balance within the cold waters of the world oceans, in *Numerical Models of Ocean Circulation*, pp. 54-56, National Academy of Science, Washington, D.C., 1975.

Harrison, K., W. Broecker, and G. Bonani, A strategy for estimating the impact of CO_2 fertilization on soil carbon storage, *Global Biogeochem. Cycles*, *7*, 69-80, 1993.

Harvey, L. D. D., Effect of model structure on response of terrestrial biosphere models to CO_2 and temperature increases, *Global Biogeochem. Cycles*, *3*, 137-153, 1989.

Hesshaimer, V., M. Heimann, and I. Levine, Radiocarbon evidence for a smaller oceanic carbon dioxide sink than previously believed, *Nature*, *370*, 201-203, 1994.

Hoffert, M.I., Global distributions of atmospheric carbon dioxide in the fossil fuel era: A projection, *Atmos. Environ.*, *8*, 1225-1249, 1974.

Hoffert, M.I., and B.P. Flannery, Model projections of the time-dependent response to increasing carbon dioxide, in Projecting the Climatic Effects of Increasing Carbon Dioxide, *Rep. DOE/ER-0237*, edited by M.C. MacCracken and F.M. Luther, pp. 149-190, U.S. Dept. of Energy, Off. of Energy Res., Washington, D.C., 1985.

Hoffert, M.I., Y.-C. Wey, A.J. Callegari, and W.S. Broecker, Atmospheric response to deep-sea injections of fossil-fuel carbon dioxide, *Clim. Change, 2*, 53-68, 1979.

Hoffert, M.I., A.J. Callegari, and C.-T. Hsieh, The role of deep sea storage in the secular response to climatic forcing, *J. Geophys. Res., 85*, 6667-6679, 1980.

Hoffert, M. I., A. J. Callegari, and C. T. Hseih, A box-diffusion carbon cycle model with upwelling, polar bottom water formation and a marine biosphere, in *Carbon Cycle Modeling*, Scope 16, edited by B. Bolin, pp. 287-305, John Wiley, New York, 1981.

Houghton, J. T., G.J. Jenkins, and J.-J. Ephraums, (Eds.), *Climatic Change: The IPCC Scientific Asessment*, Cambridge University Press, New York, 1990.

Joos, F., Imbalance in the budget, *Nature, 370*, 181-182, 1994.

Keeling, C.D., The carbon dioxide cycle: Reservoir models to depict the exchange of atmospheric carbon dioxide with the oceans and land plants, in *Chemistry of the Lower Atmosphere*, edited by S.I. Rasool, pp. 251-329, Plenum, New York, 1973.

Keeling, C. D., Impact of industrial gases on climate, in *Energy and Climate*, pp. 72-91, Geophysics Study Committee, National Academy of Sciences, Washington, D.C., 1977.

Keeling, C. D., R.B. Bacastow, A.F. Carter, S.C. Piper, T.P. Whorf, M. Heimann, W.G. Mook, and H. Roeloffzen, A three-dimensional model of atmospheric CO_2 transport based on observed winds, 1, Analysis of observational data, in *Aspects of Climate Variability in the Pacific and Western Americas, Geophys. Monogr. Ser.*, vol. 55, edited by D.H. Peterson, pp. 165-236, AGU, Washington, DC, 1989a.

Keeling, C. D., S.C. Piper, and M. Heimann, A three-dimensional model of atmospheric CO_2 transport based on observed winds, 4, Mean annual gradients and interannual variations, in *Aspects of Climate Variability in the Pacific and Western Americas, Geophys. Monogr. Ser.*, vol. 55, edited by D.H. Peterson, pp. 305-363, AGU, Washington, D.C., 1989b.

Keir, R.S., On the late Pleistocene ocean geochemistry and circulation, *Paleoceanography, 3*, 443-445, 1988.

Keir, R.S., Paleoproduction and atmospheric CO_2 based on ocean modeling, in *Productivity of the Ocean: Past and Present*, edited by W.H. Berger, V.S. Smetacek and G. Wefer, pp. 395-406, John Wiley, New York, 1989.

Kheshgi, H. S., B.P. Flannery, and M.I. Hoffert, Marine biota effects on the compositional structure of the world oceans, *J. Geophys. Res., 96*, 4957-4969, 1991.

Knox, F., and M. McElroy, Changes in atmospheric CO_2: Influence of the marine biota at high-latitudes, *J. Geophys. Res., 89*, 4629-4637, 1984.

Kohlmaier, G. H., R. Revelle, C.D. Keeling, and S.C. Piper, Reply to Idso, *Tellus, 43*B, 342-346, 1991.

Kraus, E.B., Diapycnal mixing, in *Climate-Ocean Interaction*, edited by M.E. Schlesinger, pp. 269-293, Kluwer, Norwell, Mass., 1990.

Levitus, S., Climatological Atlas of the World Ocean, *NOAA Prof.* Paper *13*, Geophy. Fluid Dyn. Lab., Princeton, N.J., 1982.

Machta, L., The role of the oceans and biosphere in the carbon cycle, in *The Changing Chemistry of the Oceans*, edited by D. Dryssen and D. Jagner, pp. 121-145, Wiley-Interscience, New York, 1973.

Maier-Reimer, E., and R. Bacastow, Modeling of geochemical tracers in the ocean, in *Climate-Ocean Interaction*, edited by M.E. Schlesinger, pp. 233-267, Kluwer Academic Norwell, Mass., 1990.

Maier-Reimer, E., and K. Hasselmann, Transport and storage of CO_2 in the ocean–An inorganic ocean-circulation carbon cycle model, *Clim. Dyn., 2*, 63-90, 1987.

Maier-Reimer, E., U. Mikolajewicz, and K. Hasselmann, Mean circulation of the Hamburg LSG OGCM and its sensitivity to the thermohaline surface forcing, *J. Phys. Oceanogr., 23*, 731-757, 1993.

Munk, W.H., Abyssal recipes, *Deep Sea Res., Oregnogr. Abstr., 13*, 707-736, 1966.

Najjar, R. G., J.L. Sarmiento, and J.R. Toggweiler, Downward transport and fate of organic matter in the ocean: Simulations with the general circulation model, *Global Biogeochem. Cycles, 6*, 45-76, 1992.

Oeschger, H., U. Siegenthaler, U. Schotterer, and A. Guglemann, A box-diffusion model to study the carbon dioxide exchange in nature, *Tellus, 27*, 168-192, 1975.

Peng, T.-H., T. Takahashi, W.S. Broecker, and J. Olafsson, Seasonal variability of carbon dioxide, nutrients and oxygen in the northern North Atlantic surface water, *Tellus, Ser. B, 39*, 439-458, 1987.

Redi, M.N., Oceanic isopycnal mixing by coordinate rotation, *J. Phys. Oceanogr., 12*, 1154-1158, 1982.

Revelle, R., and H.E. Suess, Carbon dioxide exchange bewteen the atmosphere and the ocean and the question of an increase of CO_2 during the past decades, *Tellus, 9*, 18-27, 1957.

Sarmiento, J. L., Three-dimensional ocean models for predicting the distribution of CO_2 between the ocean and atmosphere, in *The Changing Carbon Cycle*, edited by J.R. Trabalka and D.E. Reichle, pp. 279-294, Springer-Verlag, New York, 1986.

Sarmiento, J. L., and E.T. Sundquist, Revised budget for the oceanic uptake of anthropogenic carbon dioxide, *Nature, 356*, 589-593, 1992.

Sarmiento, J. L., and J.R. Toggweiler, A new model for the role of the oceans in determining atmospheric PCO_2, *Nature, 308*, 621-624, 1984.

Sarmiento, J. L., C.G.H. Rooth, and W.S. Broecker, Radium 228 as a tracer of basin wide processes in the abyssal ocean, *J. Geophys. Res., 87*, 9694-9698, 1982.

Sarmiento, J.L., J.C. Orr, and U. Siegenthaler, A perturbation simulation of CO_2 uptake in an ocean general circulation model, *J. Geophys. Res., 97*, 3621-3645, 1992.

Sarmiento, J. L., R.D. Slater, M.J.R. Fasham, H.W. Ducklow, J.R. Toggweiler and G.T. Evans, A seasonal three-dimensional ecosystem model of nitrogen cycling in the North Atlantic euphotic zone, *Global Biogeochem. Cycles, 7*, 417-450, 1993.

Schimel, D., I. Enting, M. Heimann, T. Wigley, D. Raynaud, D. Alves, and U. Siegenthaler, The carbon cycle, in *The IPCC 1994 Report on Radiative Forcing of Climate Change*, edited by J.T. Houghton, B.A. Callander, and S.K. Varney, in press, 1994.

Schlesinger, W. H., *Biogeochemistry: An Analysis of Global Change*, Academic, San Diego, Calif., 1991.

Semtner, A.J., and R.M. Chervin, Ocean general circulation from a global eddy-resolving model, *J. Geophys. Res., 97*, 5493-5550, 1992.

Shaffer, G., A model of biogeochemical cycling of phosphorous, nitrogen, oxygen, and sulfur in the ocean: One step toward a global climate model, *J. Geophys. Res., 94*, 1979-2004, 1989.

Shaffer, G. and J.L. Sarmiento, Biogeochemical cycling in the global ocean, 1, A new analytical model with continuous vertical resolution and high-latitude dynamics, *J. Geophys. Res.*, in press, 1994.

Siegenthaler, U., Uptake of excess CO_2 by an Outcrop-Diffusion Model of the ocean, *J. Geophys. Res.*, *88*, 3599-3608, 1983.

Siegenthaler, U. and F. Joos, Use of a simple model for studying oceanic tracer distribution and the global carbon cycle, *Tellus, Ser. B*, 44, 186-207, 1992.

Siegenthaler, U., and H. Oeschger, Predicting future atmospheric carbon dioxide levels, *Science*, *199*, 388-395, 1978.

Siegenthaler, U., and H. Oeschger, Biospheric CO_2 emissions during the past 2000 years reconstructed by deconvolution of ice coredata, *Tellus, Ser. B, 39*, 140–154, 1987.

Siegenthaler, U. and J.L. Sarmiento, Atmospheric carbon dioxide and ocean, *Nature*, *365*, 119-125, 1993.

Siegenthaler, U., and T. Wenk, Rapid atmospheric CO_2 variations and ocean circulation, *Nature*, *308*, 624-626, 1984.

Stevenson, F.J., and E.T. Elliott, Methodologies for assessing the quantity and quality of soil organic matter, in *Dynamics of Soil Organic Matter in Tropical Ecosystems*, edited by D.C. Coleman, J.M. Oades, and G. Vehara, pp. 173–242, University of Hawaii Press, Honolulu, 1990.

Stuiver, M., and H. Pollach, Discussion reporting of ^{14}C data, *Radiocarbon*, *19*, 355-363, 1977.

Stuiver, M., and P.D. Quay, Changes in atmospheric ^{14}C attributed to variable Sun, *Science*, *207*, 11-19, 1980.

Stuiver, M., and P.D. Quay, Atmospheric ^{14}C changes resulting from fossil fuel CO_2 release and cosmic ray flux variability, *Earth Planet. Sci. Lett.*, *53*, 349-362, 1981.

Suess, H. E., Radiocarbon concentration in modern wood, *Science*, *122*, 415-417, 1955.

Sundquist, E.T., Geological perspectives on carbon dioxide and the carbon cycle, in *The Carbon Cycle and Atmospheric CO_2: Natural Variations Archean to Present, Geophys. Monogr. Ser.*, vol. 32, edited by E.T. Sundquist, W.S. Broecker, pp. 5-59, AGU, Washington, D.C., 1985.

Takahashi, T., W. S. Broecker, and A. E. Bainbridge, Supplement to the alkalinity and total carbon dioxide concentration in the world oceans, in *Carbon Cycle Modeling*, Scope 16, edited by B. Bolin, pp. 159-199, John Wiley, New York, 1981.

Tans, P. P., A compilation of bomb ^{14}C data for use in global carbon cycle models, in *Carbon Cycle Modeling*, Scope 16, edited by B. Bolin, pp. 131-158, John Wiley, New York, 1981.

Tans, P. P., I. Y. Fung, and T. Takahashi, Observational constraints on the global atmsopheric CO_2 budget, *Science*, *247*, 1431-1438, 1990.

Toggweiler, J. R., and B. Samuels, New radiocarbon constraints on the upwelling of abyssal water to the ocean's surface, in *The Global Carbon Cycle, NATO ASI Ser.*, vol. I-15, edited by M. Heimann, pp 333-366, Spring-Verlag, New York, 1993.

Toggweiler, J.R., and J.L. Sarmiento, Glacial and interglacial changes in atmospheric carbon dioxide: The critical Role of ocean surface water in high-latitudes, in *The Carbon Cycle and Atmospheric CO_2: Natural Variations Archean to Present, Geophys. Monogr. Ser.*, vol. 32, pp. 163-184, AGU, Washington, D.C., 1985.

Toggweiler, J.R., K. Dixon, and K. Bryan, Simulations of radiocarbon in a coarse resolution world ocean model, 1, Steady state prebomb distributions, *J. Geophys. Res.*, *94*, 8217-8242, 1989a.

Toggweiler, J.R., K. Dixon, and K. Bryan, Simulations of radiocarbon in a coarse resolution world ocean model, 2, Distributions of bomb-produced carbon 14, *J. Geophys. Res.*, *94*, 8243-8264, 1989b.

Trumbore, S.E., Comparison of carbon dynamics in tropical and temprate soils using radiocarbon measurements, *Global Biogeochem. Cycles*, *7*, 275-290, 1993.

Volk, T., Multi-property modeling of the marine biosphere in relation to global climate and carbon cycles, ph.D. thesis, 348 pp., New York Univ., New York, 1984.

Volk, T., and M. I. Hoffert, Ocean carbon pumps: Analysis of relative strengths and efficiencies in ocean-driven atmospheric CO2 changes, in *The Carbon Cycle and Atmospheric CO2: Natural Variations Archean to Present, Geophys. Monogr. Ser.*, vol. 32, pp. 91-110, AGU, Washington, D.C., 1985.

Volk, T., and Z. Liu, Controls of CO_2 sources and sinks in the Earth scale surface ocean: Temperature and nutrients, *Global Biogeochem. Cycles*, 2, 73-89, 1988.

Walker, J.C.G., *Numerical Adventures with Geochemical Cycles*, 192 pp., Oxford University Press, New York, 1991.

Walker, J. C. G., and J.F. Kasting, Effect of fuel and forest conservation on future levels of atmospheric carbon dioxide, *Palaeogeogr. Palaeoclimatol. Palaeoecol.*, *97*, 151-189, 1992.

Wigley, T.M.L., A simple inverse carbon cycle model, *Global Biogeochem. Cycles, 5*, 373–381, 1991.

Wigley, T. M. L., Balancing the carbon budget: Implications for projections of future carbon dioxide concentration changes, *Tellus, Ser. B.*, 45B, 409-425, 1993.

Wyrtki, K., The oxygen minimum in relation to ocean circulation, *Deep Sea Res. Oceanogr. Abstr.*, 9, 11-23, 1961.

M.I. Hoffert, Department of Earth Systems Science, New York University, New York, NY 10003. (e-mail: hoffert@acf.nyu. edu)

A.K. Jain, and D.J. Wuebbles, University of Illinois, Department of Atmospheric Sciences, 105 S. Gregory Avenue, Urbana, IL 61801. (e-mail: jain@uiatma.atmos.uiuc.edu;e-mail: wuebbles@uiatma.atmos.uiuc.edu)

H.S. Kheshgi, Exxon Research and Engineering Company, Route 22 East, Annandale, NJ 08801.

(Received March 30, 1994; revised September 7, 1994; accepted Sepetember 14, 1994.)